LA-UR- 08-7850

Approved for public release; distribution is unlimited.

Title: Reconstructing Cosmological Matter Perturbations Using Standard Candles and Rulers

Author(s): Ujjaini Alam, LANL/ISR-1
Varun Sahni, IUCAA, Pune
Alexei Starobinsky, Landau Institute, Moscos

Intended for: Journal of Cosmology and Astroparticle Physics

Los Alamos
NATIONAL LABORATORY
EST. 1943

Reconstructing Cosmological Matter Perturbations using Standard Candles and Rulers

Ujjaini Alam[a], Varun Sahni[b] and Alexei A. Starobinsky[c,d]
[a] *Los Alamos National Laboratory, Los Alamos, USA*
[b] *Inter-University Centre for Astronomy and Astrophysics, Pune 411 007, India*
[c] *Landau Institute for Theoretical Physics, Moscow 119334, Russia and*
[d] *RESCEU, Graduate School of Physics, The University of Tokyo, Tokyo 113-0033, Japan*

For a large class of dark energy models, for which the effective gravitational constant is indeed a constant, knowledge of the expansion history suffices to reconstruct the growth factor of linearized density perturbations in the non-relativistic matter component on scales much smaller than the Hubble distance. In this paper we develop a non-parametric method for extracting information about the perturbative growth factor from data pertaining to the luminosity or angular size distances. A comparison of the reconstructed density contrast with observations of large scale structure and gravitational lensing can help distinguish DE models, such as a cosmological constant and quintessence, from modified gravity theories including Braneworlds, $f(R)$ gravity, etc. We show that for current SNe data, the instantaneous linear growth factor at $z = 0.3$ can be constrained to 5%. With future SNe data, such as expected from the JDEM mission, we may be able to constrain the growth factor to $2-3\%$ with this unbiased, model-independent reconstruction method. For future BAO data which would deliver measurements of both the angular diameter distance and Hubble parameter, it should be possible to constrain the growth factor at $z = 2.5$ to 9%. These constraints grow tighter with the errors on the datasets. With a large quantity of data expected in the next few years, this method can emerge as a competitive tool for distinguishing between different models of dark energy.

I. INTRODUCTION

Over the last decade, observations of Type Ia supernovae have shown that the expansion of the universe is currently accelerating [1, 2]. This remarkable discovery has led cosmologists to hypothesize the presence of dark energy (DE), a negative pressure energy component which dominates the energy content of the universe at present. Many theories have been propounded to explain this phenomenon, the simplest of which is the cosmological constant Λ, with constant energy density and equation of state $w = -1$. Although Λ appears to explain all current observations satisfactorily, to do so its value must necessarily be very small $\Lambda/8\pi G \simeq 10^{-47}\mathrm{GeV}^4$. So, it represents a new small constant of nature in addition to those known from elementary particle physics. However, since it is not known at present how to derive Λ from these other small constants and it is also unclear if DE is in fact time independent, other phenomenological explanations for cosmic acceleration have been suggested. These are based either on the introduction of new physical fields (quintessence models, Chaplygin gas, etc.), or on modifying the laws of gravity and therefore the geometry of the universe (scalar-tensor gravity, $f(R)$ gravity, higher dimensional 'Braneworld' models e.t.c.) (see reviews [3, 4]. The plethora of competing dark energy models has led to the development of parametric and non-parametric methods as a means of obtaining model independent information about the nature of dark energy directly from observations [5–7].

The next decade will see the emergence of many new cosmological probes. A large number of these are likely to make important contributions to the field of dark energy. The Sloan Digital Sky Survey began its stage III observations in 2008, and its Baryon Oscillation Spectroscopic Survey (BOSS) is expected to map the spatial distribution of luminous galaxies and quasars and to detect the characteristic scale imprinted by baryon acoustic oscillations in the early universe [8]. The Joint Dark Energy Mission (JDEM) is expected to discover a large number of supernovae, and also provide important data on weak-lensing and baryon acoustic oscillations [9]. The Square Kilometer Array (SKA) will map out over a billion galaxies to redshift of about 1.5, and is expected to determine the power spectrum of dark matter fluctuations as well as its growth as a function of cosmic epoch [10]. Important clues to the growth of structure will therefore come from future weak lensing surveys (JDEM, SKA, LSST) as well as redshift space distortions [11, 12] and galaxy peculiar velocities [13]. With the wealth of data expected to arrive over the next several years, it is important to explore different methods of analyzing these datasets in order to extract the optimum amount of information from them. In this paper we explore the possibility of reconstructing the linearized growth rate of density perturbations in the non-relativistic matter component, $\delta(z)$, from datasets which have traditionally been used to explore only the smooth background universe, e.g. supernova and baryon acoustic oscillations data.

In the case of *physical* DE, (when the effective gravitational constant appearing in the equation for linear density perturbations in the matter component coincides with the Newton gravitational constant G measured in the laboratory and using Solar system tests), the density contrast reconstructed in this manner should match that determined directly from observations of large scale structure. In this case the methods developed in this paper will provide an important consistency check on DE models such as Λ and Quintessence. On the other hand, *geometrical* models of DE (Braneworlds, scalar-tensor gravity, etc.) usually predict a different growth rate for $\delta(z)$ from that in general relativity. In this case, a reconstruction of the linearized density contrast from observations of standard candles/rulers will not match with δ determined directly from large scale structure. Currently reconstructed values of the growth rate from galaxy redshift distortions [11, 14, 15] are not very constrictive, but future mission like Euclid [16] are expected to constrain the growth rate tightly. Therefore comparing the results from future supernova data, using the methods described in this paper, and those from future large scale structure data will help address important issues concerning the nature of gravity and dark energy.

This paper is organized as follows. In section II, we describe the reconstruction technique and the data used to test this method. Section III shows the results and examines the dependence of the results on various factors such as the redshift distribution of the data and information on other cosmological parameters. The conclusions are presented in section IV.

II. METHODOLOGY

In the longitudinal (quasi-Newtonian) gauge, the perturbed, spatially flat, Friedman-Robertson-Walker (FRW) metric is defined by the line element

$$ds^2 = -(1+2\phi)dt^2 + (1-2\psi)a^2(t)d\vec{x}^2 \ , \tag{1}$$

where $\phi = \psi$ in general relativity (GR) if matter is free of anisotropic stresses. The Newtonian potential ϕ and the density contrast

$$\delta_m = \frac{\rho_m(\vec{x},t) - \bar{\rho}(t)}{\bar{\rho}(t)}, \tag{2}$$

are linked via the linearized Poisson equation

$$k^2\phi = -4\pi G a^2 \rho_m \delta_m \ . \tag{3}$$

It is easy to show that, on scales much smaller than the Hubble scale, the linearized growth factor for matter density perturbations in an FRW universe containing dark energy with an arbitrary effective equation of state but with the effective sound velocity $c_s \sim 1$, satisfies the equation [5, 17]

$$\ddot{\delta}_m + 2H\dot{\delta}_m - 4\pi G\rho_m\delta_m = 0 \ , \tag{4}$$

where $H(z) \equiv \dot{a}/a$ is the Hubble parameter. (We ignore the subscript in δ_m in the ensuing discussion.) The coordinate distance

$$E = \int_t^{t_0} \frac{dt}{a(t)} \equiv \int_0^z \frac{dz}{H(z)} \tag{5}$$

plays a key role in measurements of the background universe using standard rulers and candles, since

$$E(z) = \frac{d_L(z)}{1+z} = (1+z)d_A(z) \ , \tag{6}$$

where d_L and d_A are, respectively, the luminosity distance and the angular size distance. Rewriting Eq (4) in terms of Eq (5), we obtain a set of integral equations for $\delta(E)$ and its first derivative [4]:

$$\delta(E) \ = \ 1 + \delta_0' \int_0^E [1+z(E_1)]dE_1 + \frac{3}{2}\Omega_{0m} \int_0^E [1+z(E_1)] \left(\int_0^{E_1} \delta(E_2)dE_2 \right) dE_1 \tag{7}$$

$$\delta'(E) \ = \ \delta_0'[1+z(E)] + \frac{3}{2}\Omega_{0m}[1+z(E)] \int_0^E \delta(E_1)dE_1 \ , \tag{8}$$

where all derivatives are with respect to $E(z)$ and δ is normalized to $\delta(z=0)=1$. Note the remarkable fact that, in constrast to formulas used in the reconstruction of $H(z)$ from $d_L(z)$ [5, 6] or $\delta(z)$ [5] which require taking a derivative of observational data with respect to the redshift, this formula contains integrations of observational data only, which is a valid operation for noisy data.

By solving the above equations we can calculate the linear *growth factor*

$$g(z) \equiv (1+z)\delta(z) , \tag{9}$$

which represents the ratio of $\delta(z)$ in the presence of dark energy to that in SCDM without a cosmological constant. Another quantity of interest is the *growth rate*

$$f(z) = \frac{d\ln\delta}{d\ln a} = -\frac{1+z}{H(z)}\frac{d\ln\delta}{dz}. \tag{10}$$

To solve Eq (7) we start with initial guess values for $\delta(E)$ and $\delta'(E)$ and iteratively solve for $\delta(E)$, calculating $\delta'(E)$ in the successive iterations as the difference between adjacent values of $\delta(E)$, i.e. $\delta'_i = \Delta\delta_i/\Delta E_i$. This method does not require prior knowledge of the parameter δ'_0, is robust to changes in the initial guess values and gives exact results for $g(E)$ and $f(E)$ for noiseless data. For data with errors, naturally the result is noisier, however, as we will show in the succeeding sections, we will be able to put reasonable constraints on g and f using this method.

Data noise can also be decreased using smoothing techniques. In what follows we shall use the lognormal smoothing scheme proposed in [18] which has been shown to be reasonably unbiased and efficient. It constructs a smooth quantity, E^s, from a noisy one, $E(z_i)$, via the ansatz [18]

$$E^s(z) = \sum_i E(z_i)\exp\left(\frac{-\ln^2\frac{1+z_i}{1+z}}{2\Delta^2}\right) / \sum_i \exp\left(\frac{-\ln^2\frac{1+z_i}{1+z}}{2\Delta^2}\right) , \tag{11}$$

where Δ is the smoothing scale. We take $\Delta = 1/N$ where N is the total number of observations. Choosing this small value of Δ leaves the results unbiased.

Note that the equations (4) and (7) are only valid for *physical* models of dark energy such as the cosmological constant and quintessence [4]. Geometrical models of DE, which include braneworld models, scalar-tensor theories and $f(R)$ gravity, have more degrees of freedom than GR, with the result that the relation $\phi = \psi$ is usually not obeyed in such models, and the linearized perturbation equation also departs from its Newtonian form (4). For instance in extra dimensional scenario's [19], the presence of the fifth dimension (the bulk) can influence the behaviour of perturbations residing on the brane [20], whereas in scalar-tensor gravity the additional scalar degree of freedom must be taken into account when evaluating the growth of density perturbations [21]. Since, in such models, the linearized growth function $\delta_{\rm obs}(z)$ determined from observations of large scale structure would differ from its reconstructed value (7), a comparison of these two quantities could help address the important issue of whether dark energy is *geometrical* or *physical* in origin. While it is encouraging that future observations [10] of large scale structure may make possible the determination of $\delta_{\rm obs}(z)$, in this paper we focus on reconstructing this quantity using observations of high redshift type Ia supernovae and baryon acoustic oscillations.

A. Data used

The method outlined in the previous section would be applicable to any observation which contains a measurement of $E(z)$, e.g. measurements of luminosity distance or angular diameter distance. We shall use real data and mock data based on simulations of supernova type Ia data and the angular diameter distance from baryon acoustic oscillations, to test this method.

Supernova Data :

The lightcurves of Type Ia supernovae show them to be "calibrated candles", therefore they are of enormous significance in cosmology today. The luminosity distance of Type Ia SNe provide us with a direct measurement of the acceleration of the universe, thus leading to constraints on the dark energy parameters. SNe data is in the form $\{m_B, z, \sigma_{m_B}, \sigma_z\}$, where the magnitude m_B is related to $E(z)$ as

$$m_B = 5\log_{10}[(1+z)E(z)] + \mathcal{M} . \tag{12}$$

$\mathcal{M}$ is a noise parameter usually marginalized over.

Currently there are around 300 published SNe with the furthest observed one at a redshift of $z = 1.7$ [2], and average error of $\sigma_{m_B} \simeq 0.15$. Future space-based projects such as the Joint Dark Energy Mission (JDEM) [9] are expected to observe about 2000 SNe with errors of $\sigma_{m_B} = 0.07$. To date, SNe are the most direct evidence for dark

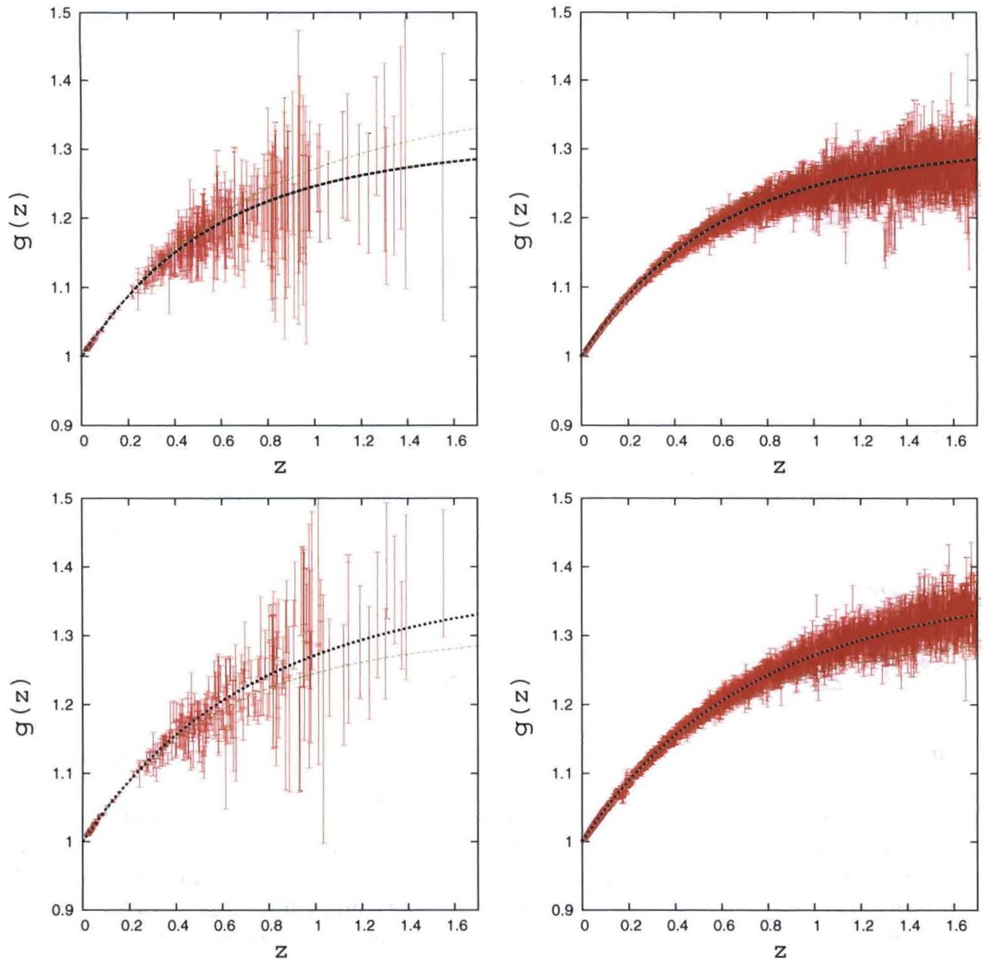

FIG. 1: Reconstructed linear growth factor $g(z)$ for different datasets. The top panels show the results for Model 1 (ΛCDM) using Union-like (set A, left panel) and JDEM-like (set B, right panel) SNe datasets, while the bottom panels show results for Model 2 (variable w, eq (13)) using set A (left panel) and set B (right panel). In each figure, the black dotted line represents the true model, while the green dashed line represents the other model. The red solid lines show the 1σ error bars for the integral reconstruction using eqs (7).

energy, and in this paper we shall primarily use SNe data to constrain the growth parameters for different dark energy models.

BAO data

At present, baryon acoustic oscillations are believed to be the method least plagued by systematic uncertainities, therefore the detection of the first baryon acoustic oscillation scale [22] has led to the speculation that BAO may in future become a potent discriminator for dark energy. Sound waves that propagate in the opaque early universe imprint a characteristic scale in the clustering of matter, providing a "standard ruler". Since the sound horizon is tightly constrained by cosmic microwave background (CMB) observations, measuring the angle subtended by this scale determines a distance to that redshift and constrains the expansion rate. The radial and transverse scales give measurements of $[r_s H(z)]/c$ and $r_s/[(1+z)d_A(z)]$ respectively, where r_s is the sound horizon obtained from CMB. These quantities are correlated, and the present BAO data is not sensitive enough to measure both quantities independently, but future surveys are expected to give independent measurements of $d_A(z)$ and $H(z)$ [23]. Future BAO surveys such as BOSS [8] are therefore expected to place tighter constraints on dark energy parameters.

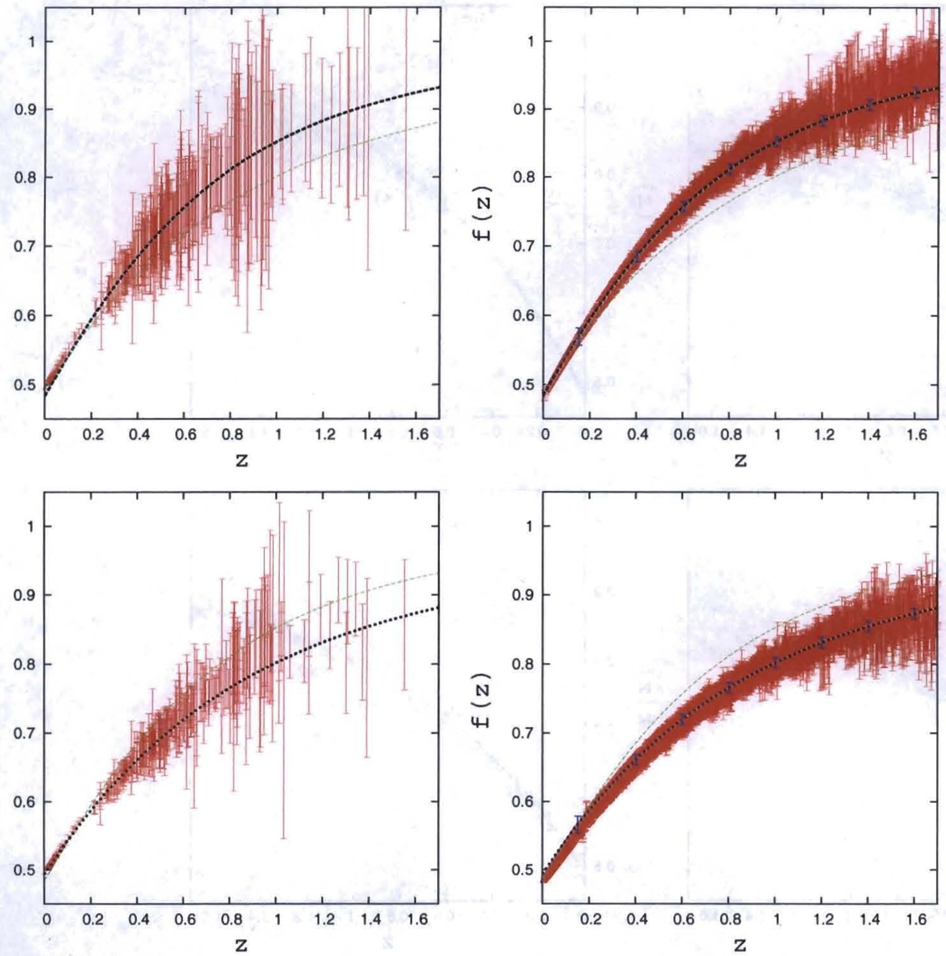

FIG. 2: Reconstructed growth rate $f(z)$ for different datasets. The top panels show the results for Model 1 (ΛCDM) using Union-like (set A, left panel) and JDEM-like (set B, right panel) SNe datasets, while the bottom panels show results for Model 2 (variable w, eq (13)) using set A (left panel) and set B (right panel). In each figure, the thick black dotted line represents the true model, while the green dashed line represents the other model. The red solid lines show the 1σ error bars for the integral reconstruction using eqs (7) The blue vertical lines in the right panel show the expected observational constraints from Euclid [16].

III. RESULTS

We first use Supernova data to reconstruct the growth parameters. We simulate data according to two theoretical models :

- Model 1 : A cosmological constant model with $w = -1, \Omega_{0m} = 0.27, H_0 = 72$ km/s/Mpc.
- Model 2: A variable dark energy model with the equation of state given by

$$w(z) = w_0 + \frac{w_a z}{1+z}, \quad w_0 = -0.9, \; w_a = 0.3 \; , \tag{13}$$

  and with the same values of Ω_{0m}, H_0 as Model 1. (Note that Model 1 and 2 provide excellent agreement with the current CMB+BAO+SNe data [24].)

Two different data distributions are used, set A resembles the quality of data available at present, and set B is modeled on expected future surveys.

- Set A : ~ 300 SNe, with the redshift distribution and errors of the Union dataset [2]. For this dataset, on average, $\sigma_{m_B} \simeq 0.15$, but a few SNe have very high errors of the order of unity. Since the method of integration

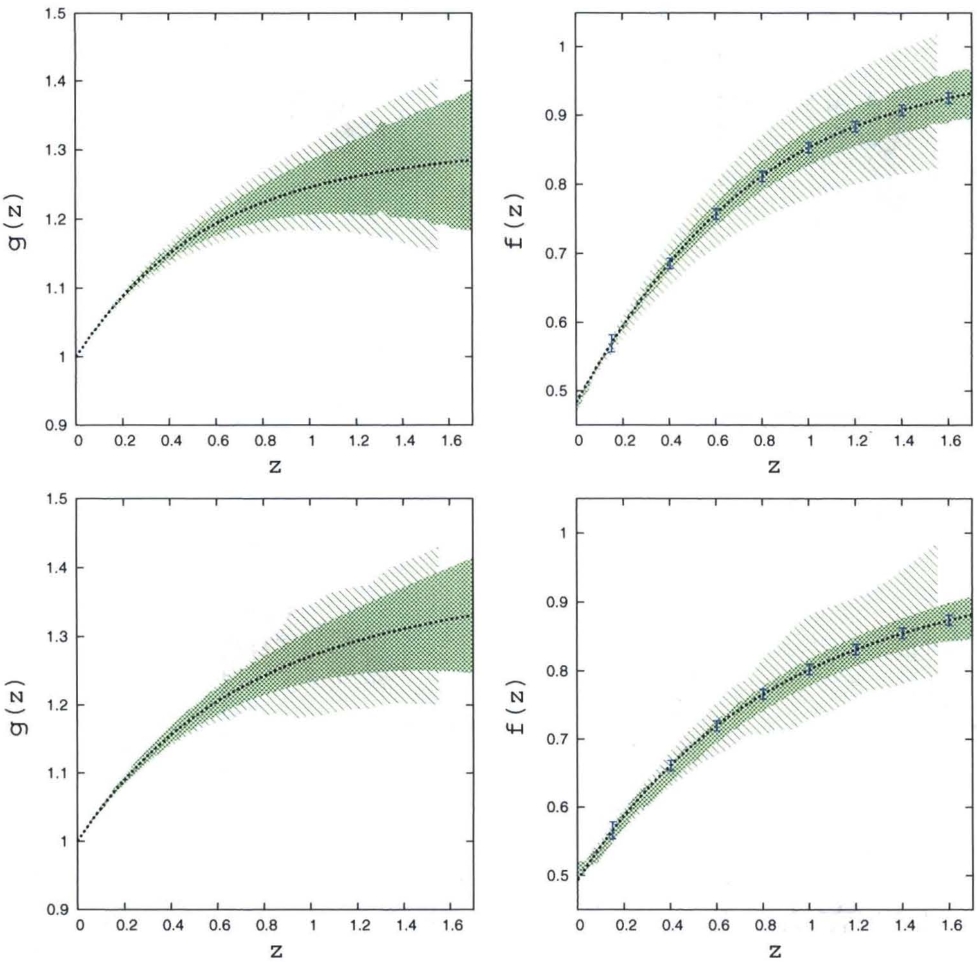

FIG. 3: Reconstructed growth parameters for different datasets using the smoothing scheme Eq (11) on the integral reconstrunction method, eq (7). The top panels show the results for Model 1 (ΛCDM) for the growth factor $g(z)$ (left panel) and the growth rate $f(z)$ (right panel). The bottom panels show the results for Model 2 (variable w, eq (13)) for $g(z)$ (left panel) and $f(z)$ (right panel). In each figure, the black dotted line represents the true model. The green dashed shaded area represents the 1σ errors for the integral reconstruction of set A (Union), while the green hatched shaded area represents the reconstruction for set B (JDEM). The blue vertical lines in the right panel show the expected observational constraints from Euclid [16].

would not work very well for very noisy data, and a single datapoint with large noise would affect the results of all datapoints after it, we restrict the analysis to SNe with $\sigma_{m_B} < 0.7$. By rejecting 10 datapoints with this criterion, we enhance the results by a significant amount.

- Set B : ~ 2000 SNe, with the redshift distribution and errors ($\sigma_{m_B} \sim 0.07$) expected from future surveys such as the JDEM [25].

For both cases, we marginalize over $\Omega_{0\mathrm{m}} = 0.27 \pm 0.03$.

Fig 1 shows the results for the linear growth factor $g(z)$ for both datasets and for the two different cosmological models. We see that for both models, set A results in rather noisy reconstruction (left panel), since the errors on the SNe are quite high. This is especially true at high redshifts ($z > 0.7$ where the sparse sampling affects the integral reconstruction scheme adversely. For JDEM-like data (set B) however, $g(z)$ is reconstructed quite accurately, and has low errors at low redshifts (right panel). At $z = 0.3$, $g(z)$ is constrained accurately to $\sim 2\%$ for both models for set B, while at $z = 1$, $g(z)$ is constrained to $\sim 4\%$.

Fig 2 shows the reconstruction of the growth rate $f(z)$. As before, the results for set A are poor. The results for Set B are reasonable, however, the errors are slightly larger in this case, since there is an additional error from the calculation of $H(z)$ from $E(z)$. At $z = 0.3$, $f(z)$ is constrained accurately to $\sim 3\%$ for both models for set B, while at $z = 1$, $f(z)$ is constrained to 8%. We also note that the quantity $f(z)$ has slightly greater discriminatory power than $g(z)$, since typically the linear growth suppresion factor shows rather less variation between different dark energy

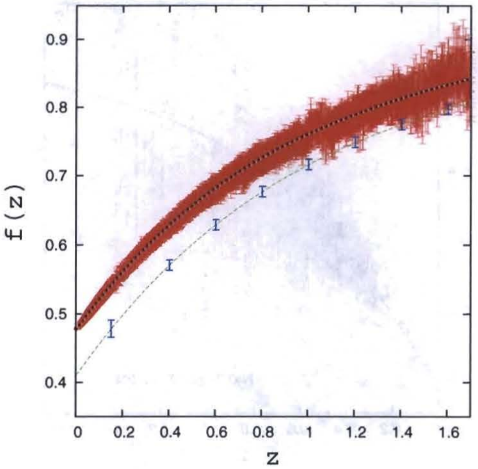

FIG. 4: Reconstructed growth rate $f(z)$ for JDEM-like dataset using a modified gravity model (DGP, eq (??)). The thick black dotted line represents the result reconstructed from just the expansion history (eq (14)), while the green dashed line represents the result reconstructed from large scale structure (eq (??)). The red solid lines show the 1σ error bars for the integral reconstruction using eqs (7) The blue vertical lines show the expected observational constraints from Euclid [16]. The discrepancy between the two would act as a signal for modified gravity.

TABLE I: Reconstructed linear growth factor g and growth rate f using different datasets for Model 1

Datasets	z	$g(z)$	$g_{\rm smooth}(z)$	$g_{\rm exact}(z)$	$f(z)$	$f_{\rm smooth}(z)$	$f_{\rm exact}(z)$
	0.3	1.11 ± 0.04	1.12 ± 0.02	1.12	0.65 ± 0.04	0.63 ± 0.03	0.64
A (Union SNe)	1.0	1.27 ± 0.06	1.26 ± 0.04	1.25	0.82 ± 0.09	0.83 ± 0.04	0.85
	1.5	1.24 ± 0.15	1.26 ± 0.09	1.28	0.97 ± 0.21	0.94 ± 0.10	0.92
	0.3	1.13 ± 0.02	1.12 ± 0.01	1.12	0.64 ± 0.02	0.63 ± 0.01	0.64
B (JDEM SNe)	1.0	1.24 ± 0.05	1.23 ± 0.04	1.25	0.86 ± 0.07	0.84 ± 0.05	0.85
	1.5	1.25 ± 0.08	1.26 ± 0.09	1.28	0.93 ± 0.11	0.92 ± 0.10	0.92
C (BOSS BAO)	2.5	1.28 ± 0.13	1.29 ± 0.11	1.30	1.01 ± 0.09	1.00 ± 0.07	0.97

models as compared to the growth rate at any given redshift. Therefore, even though $f(z)$ is slightly noisier, for set B, Model 1 and Model 2 can be discriminated at 1σ using $f(z)$.

If the data is first smoothed with the smoothing scheme (11), the results improve, especially for set A which has much noisier data, as seen in figure 3. The results for $f(z)$ improve markedly for both datasets. Errors on $g(z)$ and $f(z)$ are $\sim 1\%$ and $\sim 1.5\%$ respectively at $z = 0.3$, and $\sim 3\%$ and $\sim 6\%$ respectively at $z = 1$ for Model 1 with JDEM like data. Model 2 gives similar constraints. The results for the growth parameters are summarized in Table I for Model 1, and in Table II for Model 2. We see that this method obtains quite reasonable constraints on the growth parameters at low redshifts for the set B, therefore it can be used successfully to constrain growth parameters from

TABLE II: Reconstructed linear growth factor g and growth rate f using different datasets for Model 2

Datasets	z	$g(z)$	$g_{\rm smooth}(z)$	$g_{\rm exact}(z)$	$f(z)$	$f_{\rm smooth}(z)$	$f_{\rm exact}(z)$
	0.3	1.12 ± 0.03	1.12 ± 0.01	1.13	0.60 ± 0.04	0.61 ± 0.03	0.61
A (Union SNe)	1.0	1.26 ± 0.76	1.27 ± 0.04	1.28	0.82 ± 0.09	0.81 ± 0.07	0.80
	1.5	1.34 ± 0.18	1.33 ± 0.010	1.32	0.89 ± 0.20	0.90 ± 0.13	0.87
	0.3	1.13 ± 0.02	1.11 ± 0.01	1.13	0.62 ± 0.02	0.61 ± 0.01	0.61
B (JDEM SNe)	1.0	1.27 ± 0.05	1.27 ± 0.04	1.28	0.81 ± 0.05	0.80 ± 0.04	0.80
	1.5	1.33 ± 0.08	1.31 ± 0.07	1.32	0.88 ± 0.08	0.86 ± 0.06	0.87
C (BOSS BAO)	2.5	1.37 ± 0.13	1.346 ± 0.07	1.34	0.96 ± 0.11	0.94 ± 0.06	0.93

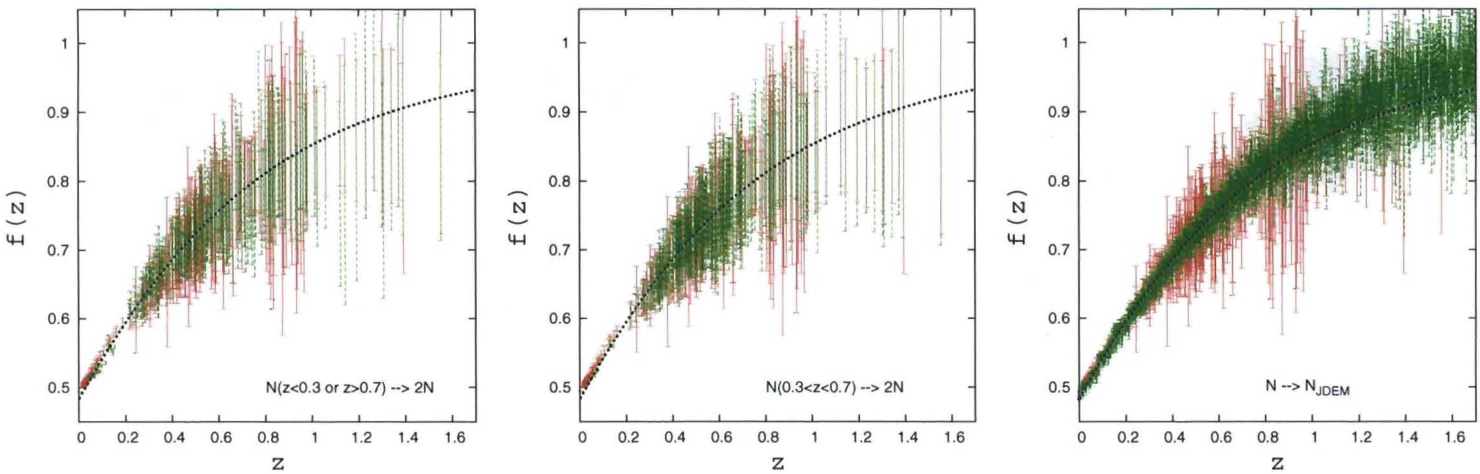

FIG. 5: Reconstructed growth rate $f(z)$ for model 1 (ΛCDM) using various redshift distributions. We use (a) set A (Union-like) with number of SNe doubled at low and high redshifts (left panel) (b) set A with number of supernova doubled for mid-range SNe (center panel) and (c) JDEM-like (set B) redshift distribution with Union-like (set A) errors (right panel). In each panel, the red solid lines depict 1σ error bars on set A, while the green dashed lines show the 1σ error bars on set A modified according to (a), (b), (c). The black dotted line represents the true model.

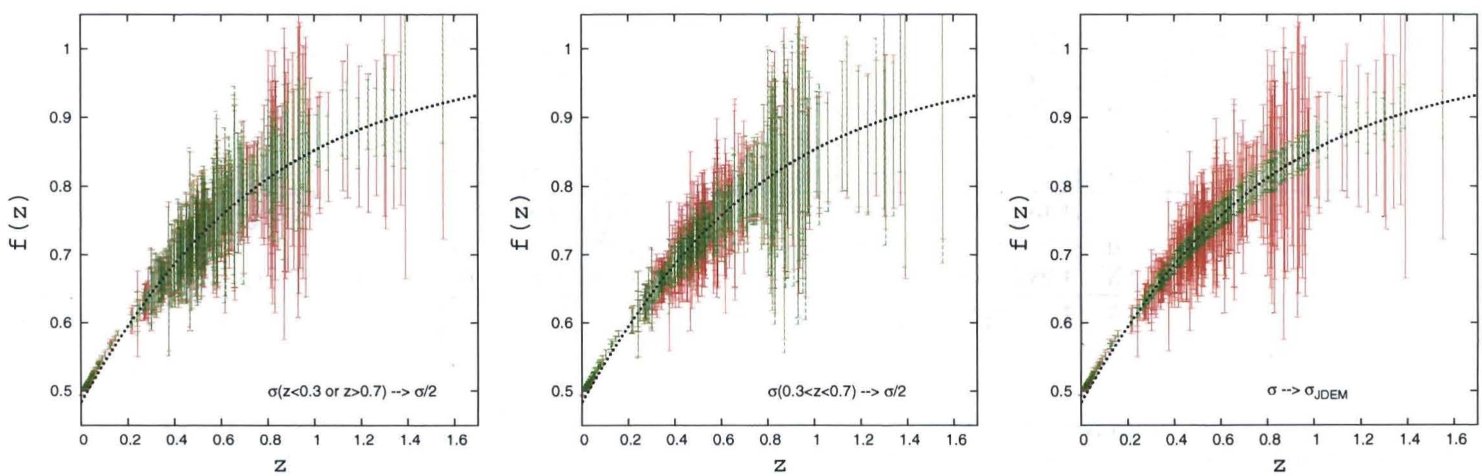

FIG. 6: Reconstructed growth rate $f(z)$ for model 1 (ΛCDM) using various error distributions. We use (a) set A (Union-like) with errors halved at low and high redshifts (left panel) (b) set A with errors halved for mid-range SNe (center panel) and (c) set A with JDEM-like errors for each SNe (right panel). In each panel, the red solid lines depict 1σ error bars on set A, while the green dashed lines show the 1σ error bars on set A modified according to (a), (b), (c). The black dotted line represents the true model.

future SNe data. It should be noted that, for future SNe data to accurately constrain the growth parameters, it is important to keep the SNe systematics under control ($\sigma_{sys} \lesssim 0.05$). A systematic error of $\sigma_{sys} = 0.1$ (as on the current data) would weaken all constraints significantly.

A. Dependence on nature of data

We now check how the results change if the redshift distribution or error distribution is changed. To study the dependency on the number of SNe, we use three redshift distributions– (a) set A (~ 300 SNe) with double the number of supernovae at low ($z < 0.3$) and high($z > 0.7$) redshifts, (b) set A with double the SNe at mid-range ($0.3 < z < 0.7$) redshifts, and (c) a distribution with the JDEM (set B) redshift distribution (~ 2000 SNe) with errors of the order of the Union (set A) SNe. The results for Model 1 are shown in figure 5. We see that doubling the number of SNe in a particular redshift bin changes the results very slightly. This is to be expected because when integrating noisy data, having a larger number of points with the same amount of noise does not improve results significantly. Increasing the total number of SNe by a significant amount (nearly seven times, as in right panel) does improve the scatter, but the results still do not compare with those of set B (fig 2, top right panel) which has the same number of supernovae but smaller errors.

We now study the effect of the errors. Once again we study three distributions — (a) set A with the errors halved for $z < 0.3$ and $z > 0.7$ redshift bins, (b) set A with errors halved in the $0.3 < z < 0.7$ redshift bin, and (c) set A with errors replaced by JDEM-like errors on all SNe. The results for Model 1 are shown in figure 6. We see that in this case, decreasing the errors at low redshift or high redshift changes the results very slightly. This is because there are very few points at low redshift so they do not affect the integration process strongly, and the high redshift points cannot affect the low redshift points. The results in the redshift range $0 < z < 0.7$ become better if the mid-range SNe have lower errors. As we see in the right panel of fig 6, decreasing the errors to JDEM errors gives results almost identical to the results for Set B (fig 2, top right panel) , even though the number of points is much less for set A. Thus we find that this method would work quite well even for a reasonable number of supernovae (of the order of a few hundred) provided the errors were tightly constrained.

Since the high errors of set A make it unsuitable for this reconstruction approach, in the next sections we will use the set B to study the robustness of the results to various other factors.

B. Growth rate from $w(z)$

We may also calculate the growth rate f from the supernova data via the equation of state using the following approximation [26] :

$$f(z) = \left(\frac{\Omega_{0\mathrm{m}}(1+z)^3}{H^2}\right)^{\Gamma(z)} \tag{14}$$

$$\Gamma(z) = \frac{3}{5-\frac{w}{1-w}} - \frac{3}{125}\frac{(1-w)(1-\frac{3}{2}w)}{(1-\frac{6}{5}w)^3}\left(1-\frac{\Omega_{0\mathrm{m}}(1+z)^3}{H^2}\right), \tag{15}$$

where the equation of state $w(z)$ may be calculated using a likelihood parameter estimation from the luminosity distance. We use the familiar parameterization [27] :

$$w(z) = w_0 + \frac{w_a z}{1+z}, \tag{16}$$

$$H^2(z) = H_0^2\left[\Omega_{0\mathrm{m}}(1+z)^3 + (1-\Omega_{0\mathrm{m}})(1+z)^{3(1+w_0+w_a)}e^{3w_a(1/(1+z)-1)}\right]. \tag{17}$$

A likelihood parameter estimation is expected to lead to smaller errors, but the drawback of this method is that the result may be biased due to the parameterization. Also the errors on $w(z)$ would propagate extremely non-linearly to f and therefore the result for $f(z)$ would be much less trustworthy.

Figure 7 shows the reconstructed $f(z)$ for Model 1 and 2 for set B. As expected, the errors are lower that those for our reconstruction method. However, it is also noteworthy that the resulting confidence levels are *not symmetric* around the true value, in fact at higher redshifts, the true model appears to be on the verge of being ruled out ! These results are commensurate with those found in [28], where reconstruction of the growth parameters through w leads to biases in the growth parameter results even though w is recovered accurately. This is due to the fact that errors propagate non-linearly from w to $f(z)$. We therefore conclude that, when reconstructing the growth parameters from supernova data, it is better to reconstruct the quantities directly, rather than reconstructing them indirectly from the energy density or equation of state.

C. Dependence on $\Omega_{0\mathrm{m}}$

Supernova data does not simultaneously constrain information on $\Omega_{0\mathrm{m}}$ and dark energy parameters. To reconstruct dark energy parameters it is necessary to place constraints on $\Omega_{0\mathrm{m}}$ from other observations. In the calculations so far, we have marginalized over the true fiducial value for $\Omega_{0\mathrm{m}}$. However, since there is considerable uncertainty as to the real value of the matter density, we check how using *incorrect* values of $\Omega_{0\mathrm{m}}$ may bias our analysis. (It is well known that an incorrect value of $\Omega_{0\mathrm{m}}$ can significantly bias the results for DE [7, 18].) The fiducial universe

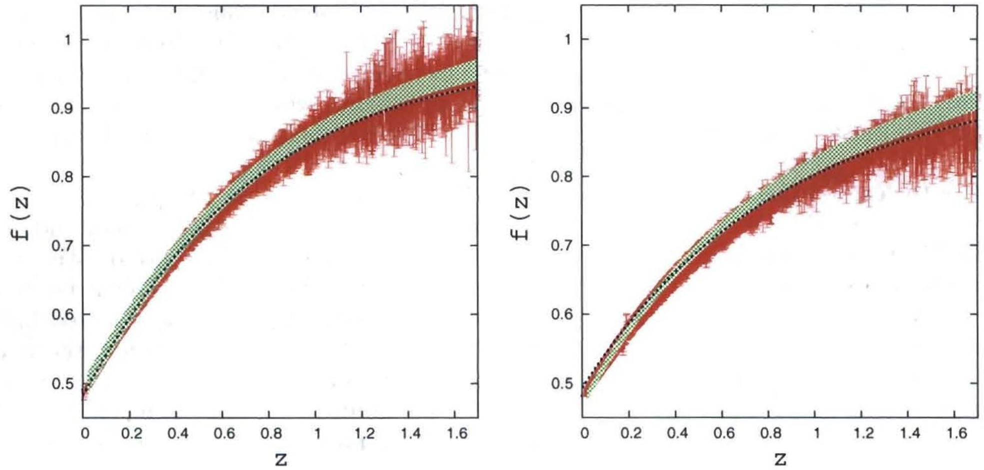

FIG. 7: Reconstructed growth rate $f(z)$ for model 1 (left panel) and model 2 (right panel) using set B (JDEM) with different reconstruction methods. The red solid lines show the 1σ limits for reconstructed $f(z)$ using the integral reconstruction method, eq (7), while the green hatched region shows the 1σ limits for $f(z)$ using w parameterization, eqs (14), (16). The black dotted line represents the true model.

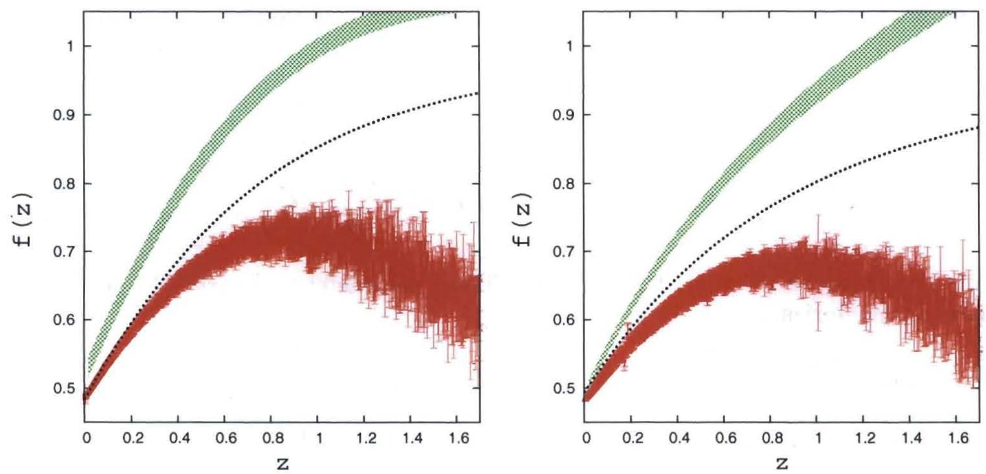

FIG. 8: Reconstructed growth rate $f(z)$ for model 1 (left panel) and model 2 (right panel) using set B with different reconstruction methods, using $\Omega_{0m} = \Omega_{0m}(\text{true}) + 0.03$. The red solid lines show the 1σ limits for reconstructed $f(z)$ using the integral reconstruction method, eq (7), while the green hatched region shows the 1σ limits for $f(z)$ using w parameterization, eqs (14), (16). The black dotted line represents the true model. Note that the results for the two reconstructions lie on opposite sides of the true value of $f(z)$.

for model 1 contains $\Omega_{0m} = 0.27$. We now choose a different, incorrect value of $\Omega_{0m} = 0.3$ for marginalization and proceed to analyze the data using both the integral reconstruction method and the likelihood parameter estimation of w outlined in the previous section. The results are shown in figure 8. We see that choosing a higher value of Ω_{0m} gives biased results in both methods, but interestingly enough, the biases are in *opposite directions* ! In case of the integral reconstruction method, a higher value of Ω_{0m} leads to a lower value of $f(z)$ at high redshifts, whereas for the w parameterization, a higher value of Ω_{0m} leads to a higher value of $f(z)$.

These results may be understood as follows. For the reconstruction from w, we see from eq (14) that $f(z)$ changes primarily due to the change in the matter density $\Omega_{0m}(1+z)^3$, since the value of Γ does not vary very strongly with w. Choosing a higher value of Ω_{0m} would therefore simply result in a higher value of $f(z)$. In the case of the integral reconstruction however, we see from eq (7) that both δ and δ' depend on Ω_{0m}. In δ the leading term is unity and the other two terms containing δ'_0 and Ω_{0m} are at about an order of magnitude smaller. In δ' the two terms containing δ'_0 and Ω_{0m} are of the same order, so both contribute equally to the result. Therefore increasing Ω_{0m} increases both

δ and δ', with δ' increasing by a greater amount, so the ratio between δ and δ' increases on the whole. Since $f(z)$ is the ratio of δ' to δ with a negative sign, this means that $f(z)$ decreases. Therefore, choosing a wrong value of Ω_{0m} causes the two different methods of reconstruction to be biased in different directions. This leads to the interesting conclusion that, provided other systematics are under control, comparing the integral reconstruction method with the standard likelihood estimation would give us a valuable consistency check on the accuracy of the prior chosen for Ω_{0m}.

D. Reconstruction for modified gravity

We consider a simple modified gravity model– the Dvali-Gabadadze-Porrati braneworld model [?]. The expansion history is for this model is given by

$$H(z) = H_0 \left[\left(\frac{1-\Omega_{0m}}{2} \right) + \sqrt{\Omega_{0m}(1+z)^3 + \left(\frac{1-\Omega_{0m}}{2} \right)^2} \right] . \quad (18)$$

For physical models of dark energy, the growth rate is well approximated by eqs (14), where typically $\Gamma simeq 0.55$. This equation is not valid however if the observed acceleration originates from a modification of the equations of the general theory of relativity; in the DGP braneworld theory, the growth rate is approximated by

$$f(z) = \left(\frac{\Omega_{0m}(1+z)^3}{H^2} \right)^{0.68} . \quad (19)$$

We therefore expect that if the growth rate for this model is reconstructed using on one hand, the integral reconstruction method with SNe data, and on the other hand, redshift distortions, the results will be different.

E. Current SNe Data

In figure 9 we show the reconstructed growth parameters for the currently available supernova data– the Union dataset [2]. The results are marginalized over $\Omega_{0m} = 0.26 \pm 0.03$, the currently accepted value of Ω_{0m} [29]. The nuisance parameter $\mathcal{M}$ which contains information on H_0 is also marginalized over. For the non-smoothed method, since the errors are quite large, it is difficult to put any constraints on the growth parameters. If the smoothing scheme is used, $f(z)$ may be constrained to $\sim 6\%$ at $z = 0.3$. The reconstructed $f(z)$ is commensurate with the cosmological constant model as well as Model 2 (variable w, eq (13)) used in this paper. We also show the three current observations of $f(z)$ from redshift space distortions [11, 14, 15]. The error bars on these observations are at present quite large, but it is expected that future data in this field could be comparable with our results from supernovae, thus we would be able to discern physical and geometrical DE using these different techniques. Table III shows the 1σ limits on the growth parameters for the reconstruction.

F. Data expected from future BAO experiments

We now check the method with BAO data. The SDSS baryon acoustic oscillation survey of BOSS is expected to measure the baryon acoustic oscillation power spectrum very accurately. The expected accuracy on the angular diameter distance d_A is of the order of 1.0% at $z = 0.35$, 1.1% at $z = 0.6$, and 1.5% at $z = 2:5$, with errors on H(z) of 1.8%, 1.7% and 1.5% at the same redshifts [8]. We populate a redshift range of $z = 0.2 - 2.5$ with 20 datapoints with errors based on these numbers and use this dataset to reconstruct the growth parameters. Since there are only 20 points in the dataset, and not many at very low redshifts, the integration is not very accurate even though the errors on d_A and H are small. We find that for this dataset $g(z)$ and $f(z)$ are both constrained to $\sim 9\%$ at $z = 2.5$ (see Tables I and II, bottom row). Although these errors appear to be large compared to those from the SNe data, for a high redshift of $z = 2.5$, these errors are actually commensurate to the errors from SNe. The advantage of using the BAO is that we obtain the growth parameters at a higher redshift, which is complementary to the SNe results. In the future, if systematics are controlled, and probes like JDEM are able to measure both SNe and BAO data, we should be able to obtain independent estimates of the growth parameters at both very low and very high redshifts from this method.

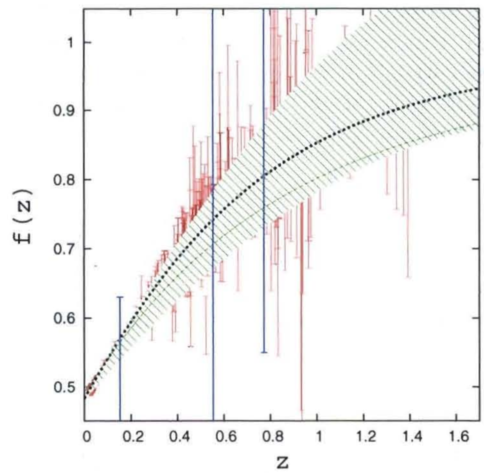

FIG. 9: Reconstructed growth rate $f(z)$ for current Union set of SNe data, using $\Omega_{0m} = 0.27 \pm 0.03$. The red solid lines show the 1σ limits for reconstructed growth parameter using the integral reconstruction method, eq (7), while the green dashed shaded area shows the 1σ limits for the parameter using smoothing scheme, eq (11), for the integral reconstruction methods. The black dotted line shows $f(z)$ for LCDM, the green dashed line shows Model 2 (variable w, eq (13)) The three vertical blue lines show the current measurements of f(z) from 2dFGRS, 2SLAQ and VVDS.

TABLE III: Reconstructed linear growth factor g and growth rate f using current supernova data

z	$g(z)$	$g_{\rm smooth}(z)$	$g_{\Lambda\rm CDM}(z)$	$f(z)$	$f_{\rm smooth}(z)$	$f_{\Lambda\rm CDM}(z)$
0.3	1.13 ± 0.05	1.13 ± 0.05	1.12	0.62 ± 0.06	0.61 ± 0.04	0.64
1.0	1.29 ± 0.10	1.28 ± 0.07	1.25	0.93 ± 0.11	0.88 ± 0.08	0.85
1.5	1.37 ± 0.16	1.35 ± 0.12	1.28	1.05 ± 0.24	0.98 ± 0.11	0.92

IV. CONCLUSIONS

In this paper we have proposed a method for extracting growth parameters for dark energy models (within the spatially flat FRW universe) from observations that map the background universe, such as measures of luminosity distance or angular diameter distance. The method is model independent and unbiased. For future JDEM SNe data, it will be able to put constraints of the order of a few percent on the growth parameters, e.g. 2% on the growth factor and 3% on the growth rate at a redshift of 0.3 , and 4% on thegrowth factor and 8% on the growth rate at a redshift of unity. In conjunction with the likelihood parameter estimation method, it acts as an important consistency check on the accuracy of the priors on Ω_{0m} for SNe. With future probes like JDEM and BOSS taken in conjunction, this method will lead to an unbiased estimation of the growth parameters upto a redshift of $z = 2.5$.

It is well known that, in GR and for most DE models, the expansion history completely determines the linearlized growth rate of density perturbations [4, 5]. Consequently, a comparison of the density contrast reconstructed from the expansion history would provide an important consistency check for a large variety of DE models including the cosmological constant and quintessence. On the other hand, a departure of the observed density contrast from that reconstructed using standard candles and rulers would almost certainly indicate one of the following:

1. A simple description of dark energy in terms of a scalar field (quintessence) or the cosmological constant is inadequate: DE may be more complicated, possessing for instance, an anisotropic stress or having interactions with dark matter.

2. Cosmic acceleration is a consequence of modified gravity. In modified gravity theories, such as Braneworld models, scalar-tensor gravity, etc., the linearized perturbation equation does not follow the Newtonian form (4). Hence the density contrast reconstructed using observations of standard candles/rulers via (4) and the density contrast determined directly from observations of large scale structure, say, by weak lensing, are likely to differ [20, 21]; also see [30] and references therein.

Future surveys such as JDEM are expected to deliver high quality data for both supernovae and weak lensing. Using such surveys it would be possible to compare the reconstructed density contrast from standard candles (SNe) with the density contrast observed from gravitational clustering (lensing). Therefore, we hope that, the techniques developed in this paper combined with future observations, will help unravel the nature of that most enigmatic quantity – dark energy.

V. ACKNOWLEDGEMENTS

AAS acknowledges RESCEU hospitality as a visiting professor. He was also partially supported by the grant RFBR 08-02-00923 and by the Scientific Programme "Astronomy" of the Russian Academy of Sciences. UA acknowledges useful discussions with S. Habib, D. Holz and Z. Lukic.

---

[1] S. J. Perlmutter, et al., 1998, Nature **391**, 51; A. G. Riess, et al., 1998, Astron. J. **116**, 1009 [astro-ph/9805201]; S. J. Perlmutter, et al., 1999, Astroph. J. **517**, 565 [astro-ph/9812133]; J. L. Tonry, et al., 2003, Astroph. J. **594**, 1, [astro-ph/0305008]; R. A. Knop, *et al.*, 2003, Astroph. J. **598**, 102 [astro-ph/0309368]; B. J. Barris, *et al.*, 2004, Astroph. J. **602**, 571 [astro-ph/0310843]; A. G. Riess, *et al.*, 2005, Astroph. J. **607**, 665 [astro-ph/0402512]; D. A. Howell, for the SNLS Collaboration, 2004, "1604-2004: Supernovae as Cosmological Lighthouses", Padua, June 16-19 2004, eds. Turatto et al., ASP conference Series. [astro-ph/0410595]; P. Astier *et al.*, 2005, Astron. Astroph. **447**, 31 [astro-ph/0510447]; A G. Riess, *et al.*, 2007, Astroph. J. **659**, 98 [astro-ph/0611572]; W. Michael Wood-Vasey, *et al.*, 2007 Astroph. J. **666**, 694 [astro-ph/0701041].

[2] M. Kowalski, *et al.*, 2008 arXiv:0804.4142.

[3] V. Sahni and A. A. Starobinsky, 2000, Int. J. Mod. Phys. **D 9**, 373 [astro-ph/9904398]; S M. Carroll, 2001, Living Rev.Rel. **4**, 1 [astro-ph/0004075]; P. J E. Peebles and B. Ratra, 2003, Rev.Mod.Phys. **75**, 559 [astro-ph/0207347]; T. Padmanabhan, 2003, Phys. Rep. **380**, 235 [hep-th/0212290]; V. Sahni, 2004, Lect. Notes Phys. **653**, 141 [astro-ph/0403324]; 2005, astro-ph/0502032; E. J. Copeland, M. Sami and S. Tsujikawa, Int. J. Mod. Phys. D **15**, 1753 (2006) [arXiv:hep-th/0603057]; S. Nojiri and S. D. Odintsov, Int. J. Geom. Meth. Mod. Phys. **4**, 115 (2007) [arXiv:hep-th/0601213]; R. P. Woodard, arXiv:astro-ph/0601672; J. A. Frieman, M. S. Turner and D. Huterer, arXiv:0803.0982; N. Straumann, arXiv:0809.5148; V. Sahni and Yu. Shtanov, arXiv:0811.3839.

[4] V. Sahni and A. A. Starobinsky, 2006, Int. J. Mod. Phys. **D 15**, 2105 [astro-ph/0610026].

[5] A. A. Starobinsky, JETP Lett. **68**, 757 (1998) [arXiv:astro-ph/9810431].

[6] D. Huterer and M. S. Turner, Phys. Rev. D **60**, 081301 (1999) [arXiv:astro-ph/9808133]; T. Nakamura and T. Chiba, Mon. Not. Roy. Ast. Soc. **306**, 696 (1999) [arXiv:astro-ph/9810447]; T. D. Saini, S. Raychaudhury, V. Sahni and A. A. Starobinsky, Phys. Rev. Lett. **85**, 1162 (2000) [arXiv:astro-ph/9910231]; T. Chiba and T. Nakamura, Phys. Rev. D **62**, 121301(R) (2000) [arXiv:astro-ph/0008175]; I. Maor, R. Brustein, J. McMahon and P. J. Steinhardt, 2002, Phys. Rev. D **65**, 123003 [astro-ph/0112526]; B. Gerke and G. Efstathiou, 2002, Mon. Not. Roy. Ast. Soc. **335**, 33 [astro-ph/0201336]; V. Sahni, T. D. Saini, A. A. Starobinsky and U. Alam, JETP Lett. **77**, 201 (2003) [arXiv:astro-ph/0201498]; P. S. Corasaniti, B. A. Bassett, C. Ungarelli and E J. Copeland, 2003, Phys. Rev. Lett. **90**, 091303 [astro-ph/0210209]; D. Huterer and G. Starkman, 2003, Phys. Rev. Lett. **90**, 031301 [astro-ph/0207517]; U. Alam, V. Sahni, T. D. Saini and A. A. Starobinsky, Mon. Not. Roy. Ast. Soc. **354** 275 (2004) [arXiv:astro-ph/0311364]; arXiv:astro-ph/0406672; U. Alam, V. Sahni and A. A. Starobinsky, JCAP **0406** 008 (2004) [arXiv:astro-ph/0403687]; Y. Wang and P. Mukherjee, 2004, Astroph. J. **606**, 654 [astro-ph/0312192]; T. D. Saini, J. Weller and S. L. Bridle, 2004, Mon. Not. Roy. Ast. Soc. **348**, 603 [astro-ph/0305526]; T. Roy Choudhury and T. Padmanabhan, 2005, Astron. Astrophys. **429**, 807 [astro-ph/0311622]; Y. Gong, 2005, Int. J. Mod. Phys. D **14**, 599 [astro-ph/0401207]; R. Lazkoz, S. Nesseris and L. Perivolaroupolos, 2005, JCAP **0511**, 010 [astro-ph/0503230]; H. K. Jassal, J. S. Bagla and T. Padmanabhan, 2005, Mon. Not. Roy. Ast. Soc. **356**, L11 [astro-ph/0404378]; Y. Wang and M. Tegmark, 2005, Phys. Rev. D **71**, 103513 [astro-ph/0501351]; R. A. Daly and S. G. Djorgovsky, 2005, astro-ph/0512576; J. Simon, L. Verde and R. Jimenez, Phys. Rev. D **71**, 123001 (2005) [arXiv:astro-ph/0412269]; Z. K. Guo, N. Ohta and Y. Z. Zhang, Phys. Rev. D **72**, 023504 (2005) [arXiv:astro-ph/0505253]; R. Lazkoz, S. Nesseris and L. Perivolaroupolos, JCAP **0511**, 010 (2005) [arXiv:astro-ph/0503230]; S. Nesseris and L. Perivolaropoulos, Phys. Rev. D **72** 123519 (2005) [arXiv:astro-ph/0511040]; S. Tsujikawa, Phys. Rev. D **72**, 083512; (2005) [arXiv:astro-ph/0508542]; D. Polarski and A. Ranquet, Phys. Lett. B **627**, 1 (2005) [arXiv:astro-ph/0507290]; Y. Wang and P. Mukherjee, Astroph. J. **650**, 1 (2006) [arXiv:astro-ph/0604051]; B. Feng, M. Li, Y-S. Piao and X. Zhang, Phys. Lett. B **634**, 101 (2006) [arXiv:astro-ph/0407432]; Z. K. Guo, N. Ohta and Y. Z. Zhang, Mod. Phys. Lett. **A22**, 883 (2007) [arXiv:astro-ph/0603109]; Y. Wang and K. Freese, Phys. Lett. B **632**, 449 (2006) [arXiv:astro-ph/0402208]; F. Simpson and S. Bridle, Phys. Rev. D **73**, 083001 (2006) [arXiv:astro-ph/0602213]; A. A. Sen, JCAP **0603**, 010 (2006) [arXiv:astro-ph/0512406]; R. Lazkoz, S. Nesseris and L. Perivolaroupolos, arXiv:0712.1232; X. Zhang, Phys. Lett. **B648**, 1 (2007) [arXiv:astro-ph/0604484]; Phys. Rev. **D74**, 103505 (2006) [arXiv:astro-ph/0609699]. R. A. Daly and S. G. Djorgovsky, arXiv:astro-ph/0609791; S. Fay and R. Tavakol, Phys.Rev. D **74** 083513 (2006) [arXiv:astro-ph/0606431]; N. Pires, Z. H. Zhu and J. S. Alcaniz, Phys. Rev. D **73** 123530 (2006); [arXiv:0706.1779 [astro-ph]]; M.A. Dan-

tas, J.S. Alcaniz, D. Jain and A. Dev, Astron. Astrophys. **467**, 421 (2007) [arXiv:astro-ph/0607060]; J. Santos, J. S. Alcaniz, M. J. Reboucas and N. Pires, Phys. Rev. D **76** 043519 (2007) [arXiv:0706.1779]; U. Alam, V. Sahni and A. A. Starobinsky, JCAP **0702** 011 (2007) [arXiv:astro-ph/0612381]; S. Nesseris and L. Perivolaropoulos, JCAP **0701** 018 (2007) [astro-ph/0610092]; E. E. O. Ishida, R. R. R. Reis, A. V. Toribio and I. Waga, Astropart. Phys. 28, 547 (2008) [arXiv:0706.0546]; R. A. Daly *et al.*, arXiv:0710.5345 [astro-ph]; L. Samushia and B. Ratra, arXiv:0803.3775 [astro-ph]; arXiv:0806.2835 [astro-ph] T. Chiba and T. Nakamura, Prog. Theor. Phys. **118**, 815 (2007) [arXiv:0708.3877]; S. Nesseris and L. Perivolaropoulos, Phys. Rev. D **77**, 023504 (2008) [arXiv:0710.1092]; D. Sarkar, *et al.*, Phys. Rev. Lett. **100**, 241302 (2008) [arXiv:0709.1150]; J.-M. Virey, *et al.*, arXiv:0802.4407; C. Zunckel and C. Clarkson, arXiv:0807.4304.

[7] V. Sahni, A. Shafieloo and A. A. Starobinsky, Phys. Rev. D **78**, 103502 (2008) [arXiv:0807.3548].

[8] http://www.sdss3.org/;
http://cosmology.lbl.gov/BOSS/;
http://www-physics.lbl.gov/physdiv/div-office/2006dirreview/Schlegel.pdf.

[9] http://universe.nasa.gov/program/probes/jdem.html

[10] C.A. Blake, F.B. Abdallah, S.L. Bridle and S. Rawlings, In "Science with the Square Kilometer Array", eds. C.Carilli and S.Rawlings, New Astronomy Reviews (Elsevier: Amsterdam) arXiv:astro-ph/0409278.

[11] L. Guzzo *et al.*, 2008, Nature **451**, 541

[12] W. J Percival and Martin White, 2008, arXiv:0808.0003.

[13] Y-S. Song and W. J. Percival, 2008, arXiv:0807.0810.

[14] L. Verde, *et al.*, 2002, Mon. Not. Roy. Ast. Soc. **335**, 432; E. Hawkins *et al.*, 2003, Mon. Not. Roy. Ast. Soc. **346**, 78.

[15] N. P. Ross, *et al.*, 2007, Mon. Not. Roy. Ast. Soc. **381**, 573.

[16] http://sci.esa.int/science-e/www/object/index.cfm?fobjectid=42266;
http://hetdex.org/otherprojects/euclid.php;
A. Cimatti *et al.*, 2008, arXiv:0804.4433.

[17] P. J. E. Peebles, 1980, *The Large scale structure of the universe*, Princeton university press; V. Sahni and P. Coles, 1995, Phys. Rept. **262**, 1 [astro-ph/9505005].

[18] A. Shafieloo, U. Alam, V. Sahni and A. A. Starobinsky, 2006, Mon. Not. Roy. Ast. Soc. **366**, 1081 [astro-ph/0505329]; A. Shafieloo, 2007, Mon. Not. Roy. Ast. Soc. **380** 1573.

[19] G. Dvali, G. Gabadadze, and M. Porrati, Phys. Lett. B **485**, 208 (2000) [hep-th/0005016]; V. Sahni and Yu. Shtanov, JCAP **0311**, 014 (2003) [astro-ph/0202346].

[20] Koyama K and Maartens R 2006 *JCAP* **0601** 016 (2006) [arXiv:astro-ph/0511634]; Koyama K 2006 *JCAP* **0603** 017 [arXiv:astro-ph/0601220]; Sawicki I, Song Y-S and Hu W 2007 *Phys. Rev.* D **75** 064002 [arXiv:astro-ph/0606285]; Yu. Shtanov, A. Viznyuk, and V. Sahni, Class. Quantum Grav. **24** (2007) 6159, [arXiv:astro-ph/0701015].

[21] B. Boisseau, G. Esposito-Farese, D. Polarski and A. A. Starobinsky, 2000, Phys. Rev. Lett. **85**, 2236 [gr-qc/0001066].

[22] D. J. Eisenstein, *et al.*, 2005, Astroph. J. **633**, 560 [astro-ph/0501171].

[23] H. S. Seo and D. J. Eisenstein, 2003, Astroph. J. **598**, 720 [astro-ph/0307460].

[24] E. Komatsu, *et al.*, arXiv:0803.0547 [astro-ph].

[25] G. Aldering *et al.*, 2004, astro-ph/0405232.

[26] L. Wang and P. J. Steinhardt, 1998, Astroph. J. **508**, 483.

[27] M. Chevallier and D. Polarski, 2001, Int. J. Mod. Phys. D **10**, 213 [gr-qc/0009008].
E. V. Linder, 2003, Phys. Rev. Lett. **90**, 091301 [astro-ph/0208512].

[28] M. J. Mortonson, W. Hu, D. Huterer, 2008, arXiv:0810.1744

[29] J. Dunkley, *et al.*, 2008, arXiv:0803.0586.

[30] B. Jain and P. Zhang, 2007, arXiv:0709.2375; G-B. Zhao, L. Pogosian, A. Silvestri and J. Zylberberg, 2008, arXiv:0809.3791; Y-S, Song and O. Dorè, 2008, arXiv:0812.0002.